'Atiqot 115, 2024

Economic Strategies of Two Early Bronze Age Villages in the Southern Levant: Explaining Coastal Abandonment Versus Inland Urban Development

Roey Nickelsberg, Anastasia Shapiro, Anat Cohen-Weinberger, Yitzhak Paz, Itai Elad, Assaf Yasur-Landau and Ruth Shahack-Gross[1]

The southern Levantine coast was settled continuously for three millennia, from the Neolithic period until its abandonment in Early Bronze Age II, in sharp contrast to inland sites that developed into urbanized cities. This study examines this phenomenon by investigating the pottery production component of the economic systems of two contemporary EB I villages: a shoreline coastal site that was abandoned (Dor South) and an inland site that evolved into an urban center ('En Esur). This pilot ceramic petrography examination shows two distinct strategies, with 'En Esur producing pottery primarily from local raw materials and Dor South relying mainly on imported pottery, potentially weakening the once-resilient coastal system.

Keywords: coastal archaeology, coastal resources, trade networks, sustainability, EB IA, Dor South, 'En Esur

Introduction

Early Bronze Age IA (c. 3700–3350 BCE; Regev et al. 2012:561) saw the final stages of village societies in the Southern Levant, with the rise of the first urban centers beginning subsequently, as early as EB IB (c. 3350/3300–3000 BCE; Paz 2002:254–255; Milevski, Liran and Getzov 2014:3). The significant shift in subsistence strategies and settlement patterns began with the transition from the Chalcolithic period, acting as a major link in the social and economic evolution. Command over local vegetal, animal and landscape resources, and the accumulation

[1] Dr. Roey Nickelsberg, Department of Maritime Civilizations, School of Archaeology and Maritime Cultures, University of Haifa, Israel; Anastasia Shapiro, Dr. Anat Cohen-Weinberger, Dr. Yitzhak Paz and Itai Elad (Ph.D candidate), Israel Antiquities Authority; Prof. Assaf Yasur-Landau and Prof. Ruth Shahack-Gross, Department of Maritime Civilizations, School of Archaeology and Maritime Cultures, University of Haifa, Israel, and The Leon Recanati Institute for Maritime Studies, University of Haifa, Israel.

of surplus, were well-established in EB IA villages, as well as craft specialization and the trade of goods, all of which were interconnected to form a sustainable economy. The settlements' inhabitants relied on local production, with what may be considered a limited hierarchical organization (Greenberg 2019:34–35), as well as on the use of pack animals, which facilitated the long-distance transportation of goods, such as basalt and copper (Milevski 2009:133; Greenberg 2019:34). Maintaining this economic strategy during the transition to urbanism in EB IB required social organization and a rearrangement of settlements in locations rich in sustainable raw materials and fertile landscapes (Chesson 2019). Examples of an early establishment of stable urban centers are Megiddo and 'En Esur, both of which present a growth of settlement and the construction of public structures, which were absent in EB IA (Adams et al. 2014; Greenberg 2019; Elad and Paz 2023). As a result of this reorganization, it appears that certain areas were abandoned, while others continued to thrive. This is best attested in the overall abandonment of the Southern Levantine coast by EB II, in contrast to the evolvement of inland sites into urbanized centers (Gophna and Portugali 1988; Faust and Ashkenazy 2009). While a reasonable explanation for settlement change is often a shift in available resources, it does not seem to be the case for the coastal plain, which has been shown to have ample natural resources that could support growing economies (Nickelsberg et al. 2024; Nickelsberg, Shahack-Gross and Yasur-Landau 2024). Since the Neolithic period, the Southern Levantine coastal plain was occupied by village societies continuously for over 3000 years, apparently resilient even in the face of climate change (Nickelsberg et al. 2024). The observed demise of the coastal settlement pattern at the end of EB IB is therefore intriguing and demands an alternative explanation.

One hypothesis tested in this research is that the abandonment of the coast was the result of a shift in economic strategy. While this shift may have occurred during EB IB, we may expect to see early signs of changing economic strategies as early as EB IA. For this, we compared the site of Dor South, a shoreline coastal site representing the latest stage of coastal villages, and the site of 'En Esur, an inland coastal plain site (Fig. 1). These sites were chosen as they are both EB IA sites in the northern coastal plain of Israel (based on pottery typology; no absolute ages available), relatively close to one another (16 km as the crow flies), and thus, sharing landscape aspects related to their economic strategies. Additionally, both sites were of about the same extent during EB IA (Elad and Paz 2018; Nickelsberg and Shahack-Gross 2021), and their pottery assemblages are similar (Elad and Paz 2018; Shahack-Gross et al. 2024), suggesting that these villages shared aspects related to pottery production and use. For example, the consistent appearance of Early Bronze Age Gray Burnished Ware (henceforth, GBW) in EB IA contexts across northern and central Israel has been suggested to indicate a new form of connectivity. Importantly though, petrographic analyses have shown that GBW vessels were produced of local raw materials, suggesting that the form of this connectivity was not trade but rather specialized craftsmen who traveled to different sites manufacturing GBW locally (Milevski 2009; Greenberg 2019).

Despite the similarities with 'En Esur, Dor South was abandoned, representing the end of the prehistoric–protohistoric coastal settlement pattern, while its counterpart developed

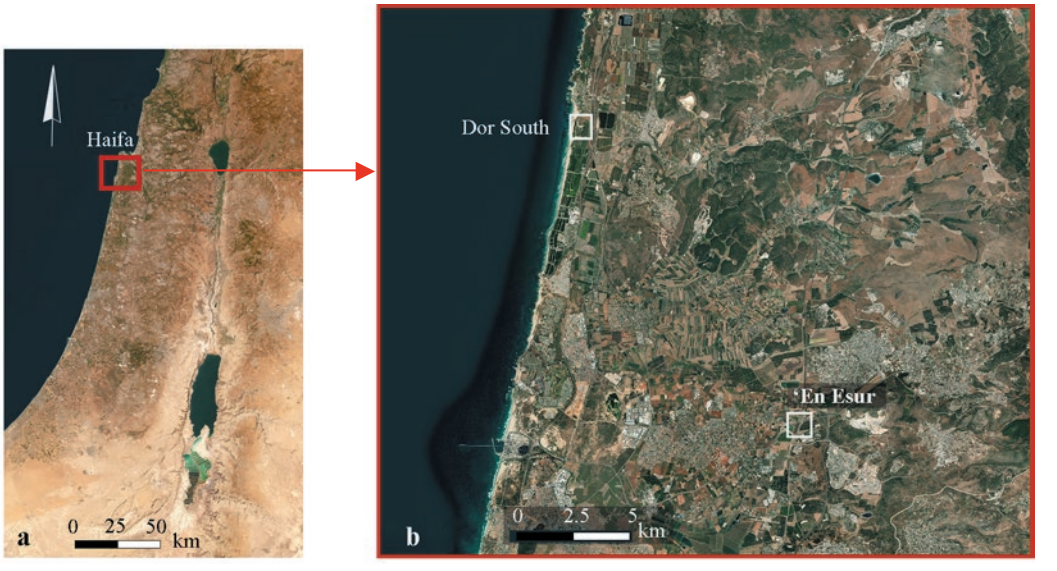

Fig. 1. Satellite image of Israel (a) and the locations of Dor South and 'En Esur (b) (created using ESRI satellite maps).

into an urban center. To test our hypothesis that this disparity was the result of a shift in economic strategies, we compared the pottery production and acquisition methods of both sites during EB IA, focusing on petrographic identification of raw materials used in ceramic production. While pottery may not represent a major component of village economy, these finds can provide significant insights into each site's economic strategy regarding a common commodity that is represented in the archaeological record.

The Study Sites: Background and Local Geological and Pedological Resources

Dor South is a narrow and long site (c. 1 km) located on the Carmel Coast. Pottery and other finds recovered during its excavation indicated occupation as early as the Pottery Neolithic. During EB IA, Dor South was a sedentary village with an agropastoral subsistence base (Nickelsberg and Shahack-Gross 2021; for a detailed pottery typology, see Shahack-Gross et al. 2024); finds from this period were unearthed throughout the site, while the EB IB presence is limited to its southernmost edge (Nickelsberg and Shahack-Gross 2021; Shahack-Gross et al. 2024). This EB I coastal site, currently positioned a few tens of meters from the shoreline, ceased to exist by EB II, conforming to our current knowledge of coastal settlement patterns (Faust and Ashkenazy 2009; Milevski 2013; Greenberg 2019:29; Nickelsberg, Shahack-Gross and Yasur-Landau 2024).

‘En Esur is located farther inland, about 12 km east of the current coastline, in the Sharon coastal plain, on the border between the Umm el-Faḥm anticline and the Menashe Hills syncline (Sass 1968). The excavations at the site revealed a small EB IA settlement that developed during early EB IB into a very large village, becoming by late EB IB an urban center that encompassed an elaborate planned street system, massively built domestic quarters, public buildings (including a monumental temple) and a fortification system (Elad and Paz 2023).

While Dor South and ‘En Esur are located relatively close to one another (Fig. 1), their geological and pedological settings are different (Fig. 2). Dor South is situated within coastal sand dunes composed of fine to medium sand-sized quartz grains typical of the region (Frechen et al. 2004). The site is bordered on the west by an aeolianite (locally termed *kurkar*) ridge, and to its east lies the Carmel coastal plain, composed of dark-brown silty clay that was formed by alluvial deposits arriving from Mount Carmel, and in antiquity also by sediment accumulation in coastal marshes (Ogloblin Ramirez, Galili and Shahack-Gross 2021). Rocks found on Mount Carmel, farther to the east, include mainly terminal Lower Cretaceous limestone and dolomite, and Upper Cretaceous chalky limestone with occasional chert nodules, interfingered with volcanic tuffs (Segev and Sass 2009; Ogloblin Ramirez, Galili and Shahack-Gross 2021). *Terra rossa* and rendzina soils occur on the carbonate rocks of Mount Carmel (Dan et al. 1975). In the south, the site borders with the mouth of Naḥal Daliya, which flows along the Menashe Hills, transporting sediments that originate in eroded Eocene chalk and chert, as well as volcanic rocks from the Shefeya region (Segev and Sass 2009; Ogloblin Ramirez et al. 2021). Accessible clay-rich raw materials for pottery production therefore include the marshy/alluvial coastal plain deposits and *terra rossa* and rendzina soils from Mount Carmel, as well as alluvial deposits associated with Naḥal Daliya. Ogloblin Ramirez et al. (2021) have presented the petrographic characteristics of these potential sources. In short, clays typical of the Carmel Coast are dominated by fine to medium-sized quartz sand, occasional *kurkar* and volcanic tuff grains and marine algae such as *Amphiroa* sp. in sources close to the shoreline.

‘En Esur is located on the Quaternary colluvial and alluvial soils of the Sharon plain, including the typical local sandy red soil, denoted as *ḥamra*, and grumusols of Naḥal ‘Iron (Ravikovitch 1969). Rocks found in the Umm el-Faḥm anticline are Cretaceous limestones, dolomites and volcanic tuffs/basalts, while the Menashe Hills lithology is of Paleocene and Eocene chalk and marl (Sass 1968). The excavated area is situated along Naḥal ‘Iron, where both alluvial deposits and *ḥamra* soil occur, associated with a *kurkar* ridge located farther to the west (Ravikovitch 1969). Chalk and chert of the Lower Eocene ‘Adulam Formation occur north and northeast of the site, while chalk and marl of the Paleocene Taqiye Formation and chalk of the Middle Eocene Maresha Formation are exposed along Naḥal ‘Iron, east of the site (Sneh et al. 1996; Segev et al. 2002:298; Sass, Dekel and Sneh 2013). Rendzina and brown forest soils are found on these soft chalky-marly rocks (Ravikovitch 1969). There are chalk and marly chalk of the Senonian Menuḥa Formation approximately one kilometer southeast of the site (Sneh et al. 1996). Accessible potential raw materials used for the paste

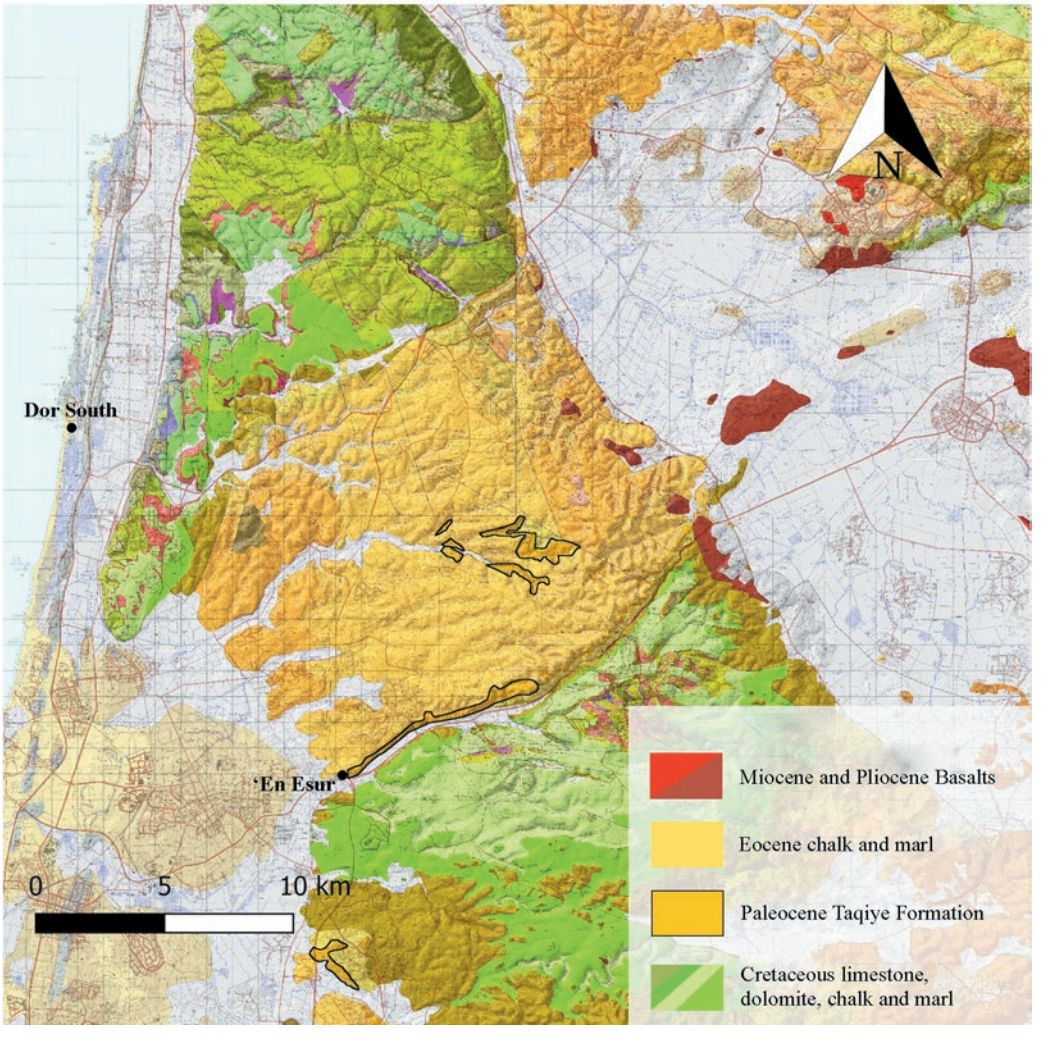

Fig. 2. Geological map of the study area; the legend refers only to geological units relevant to this research (Segev and Sass 2009; Sass et al. 2013; Sneh et al. 1996).

in the pottery production at 'En Esur therefore include *ḥamra* soil, alluvial sediments of Naḥal 'Iron, rendzina soil and marl of the Paleocene Taqiye Formation.

Materials and Methods

The pottery assemblages recovered from the EB IA phases at each site are rather similar typologically, including characteristic EB IA storage jars, pithoi, holemouth jars, GBW and red burnished ware (for the Dor South pottery typology, see Nickelsberg in Shahack-Gross et al. 2024; for the 'En Esur pottery typology, see Elad and Paz 2018).

We conducted petrographic analyses to identify the raw materials of the matrix, as well as the aplastic components of the pottery recovered at each site. A total of 35 sherds, 23 from Dor South and 12 from ‘En Esur, were analyzed, representing the main typological groups characteristic of EB IA: (A) cooking vessels, including holemouths; (B) jars; (C) GBW and (D) red burnished ware (Table 1; Figs. 3, 4). This relatively small sample size was found to be sufficient for this pilot study: results show similar intra-site clay recipes at both sites, meaning that the low petrofabric variety described below is not due to insufficient sampling but rather the result of intra-site consistency.

In the Dor South assemblage, sherds from Groups A and B comprise mainly bases, rims and handles of storage jars and holemouth vessels. The cooking vessels among these (Group A) were differentiated based on traces of soot. Group C comprises gray sherds identified as GBW based on the characteristic knob features and/or the surface treatment typical of this group. Group D, with a red-slipped and often also burnished surface, comprises storage jars, holemouth jars and bowls. Similar types were studied from ‘En Esur, including GBW, holemouth jars and necked storage jars/pithoi (Table 1). It is important to note that two sherds from the Dor South assemblage were sampled because they were suspected as being composed of a different material than the rest, based on their gritty appearance (Table 1:22, 23; Fig. 3:E). These were exceptional within an assemblage of hundreds of pottery sherds retrieved from Dor South, and were the only sherds that were selected intentionally rather than randomly.

Thin sections (30 µm thick) were prepared at the University of Haifa for the samples from Dor South, and at the Israel Antiquities Authority, for the samples from ‘En Esur. Petrographic observations were carried out using a polarized light microscope (Nikon

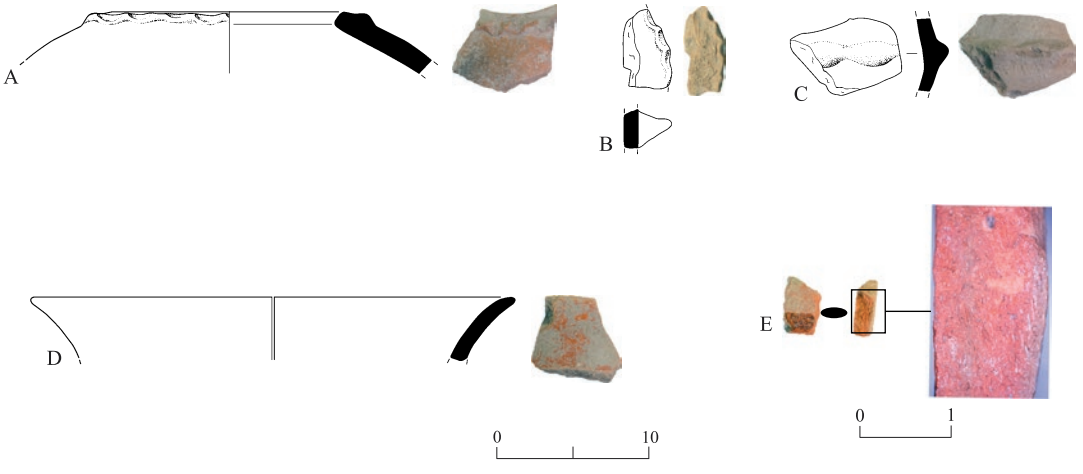

Fig. 3. Representative examples of typological pottery groups: (A) holemouth cooking pot (with soot traces) ; (B) ledge handle of a storage jar; (C) GBW sherd; (D) red burnished storage jar rim; (E) sherd with gritty paste, suspected as coastal.

Table 1. The Pottery Samples from Dor South (1–23) and ‘En Esur (24–35)

No.	Sample No.	Type[i]	Site	Locus	Basket
1	DS-1	CV	Dor South	19A6	19A6-2.1
2	DS-2	CV	Dor South	19A18	19A18-2.3
3	DS-3	CV	Dor South	19A18	19A18-2.10
4	DS-4	CV	Dor South	19A10	19A10-3.1
5	DS-5	CV	Dor South	19A18	19A18-2.11
6	DS-6	SJ	Dor South	19A16	19A16-1.5
7	DS-7	SJ	Dor South	19A18	19A18-2.1
8	DS-8	SJ	Dor South	19A22	19A22-1.1
9	DS-9	SJ	Dor South	19A14	19A14-3.5
10	DS-10	SJ	Dor South	19A14	19A14-3.3
11	DS-11	GBW	Dor South	19A6	19A6-2.2
12	DS-12	GBW	Dor South	19A7	19A7-3.4
13	DS-13	GBW	Dor South	19A14	19A14-2.3
14	DS-14	GBW	Dor South	19A16	19A16-1.2
15	DS-15	GBW	Dor South	19A10	19A10-1.1
16	DS-16	RB	Dor South	19A11	19A11-1.6
17	DS-17	RB	Dor South	19A5	19A5-2.2
18	DS-18	RB	Dor South	19A10	19A10-2.1
19	DS-19	RB	Dor South	19A11	19A11-1.7
20	DS-20	RB	Dor South	19A5	19A5-1.1
21	DS-21	RB	Dor South	19A4	19A5-2.6
22	DS-22	Body sherd[ii]	Dor South	19A15	19A15-1.1
23	DS-23	Body sherd[ii]	Dor South	19A22	19A22-3.1
24	En Esur-17.3	GBW	‘En Esur	51054	510220/1
25	En Esur-19.3	Pithos	‘En Esur	50470	502002/2
26	En Esur-17.4	GBW	‘En Esur	52067	520700
27	En Esur-17.2	GBW	‘En Esur	52024	520166/3
28	En Esur-18.2	HM/CV	‘En Esur	51054	520220/4
29	En Esur-17.6	HM/CV	‘En Esur	50465	502843/2
30	En Esur-18.4	HM/CV	‘En Esur	50465	502843/3
31	En Esur-18.1	HM/CV	‘En Esur	50537	503511/2
32	En Esur-19.1	SJ	‘En Esur	52036	520371/3
33	En Esur-18.5	SJ	‘En Esur	52054	520220
34	En Esur-17.5	HM/CV	‘En Esur	52054	520220/2
35	En Esur-19.2	Pithos	‘En Esur	50327	503308/5

[i] Abbreviations: CV = cooking vessel; SJ = storage jar; GBW = Gray Burnished Ware; RB = red burnished; HM = holemouth jar.

[ii] Body sherds that were suspected as coastal material and selected for analysis intentionally.

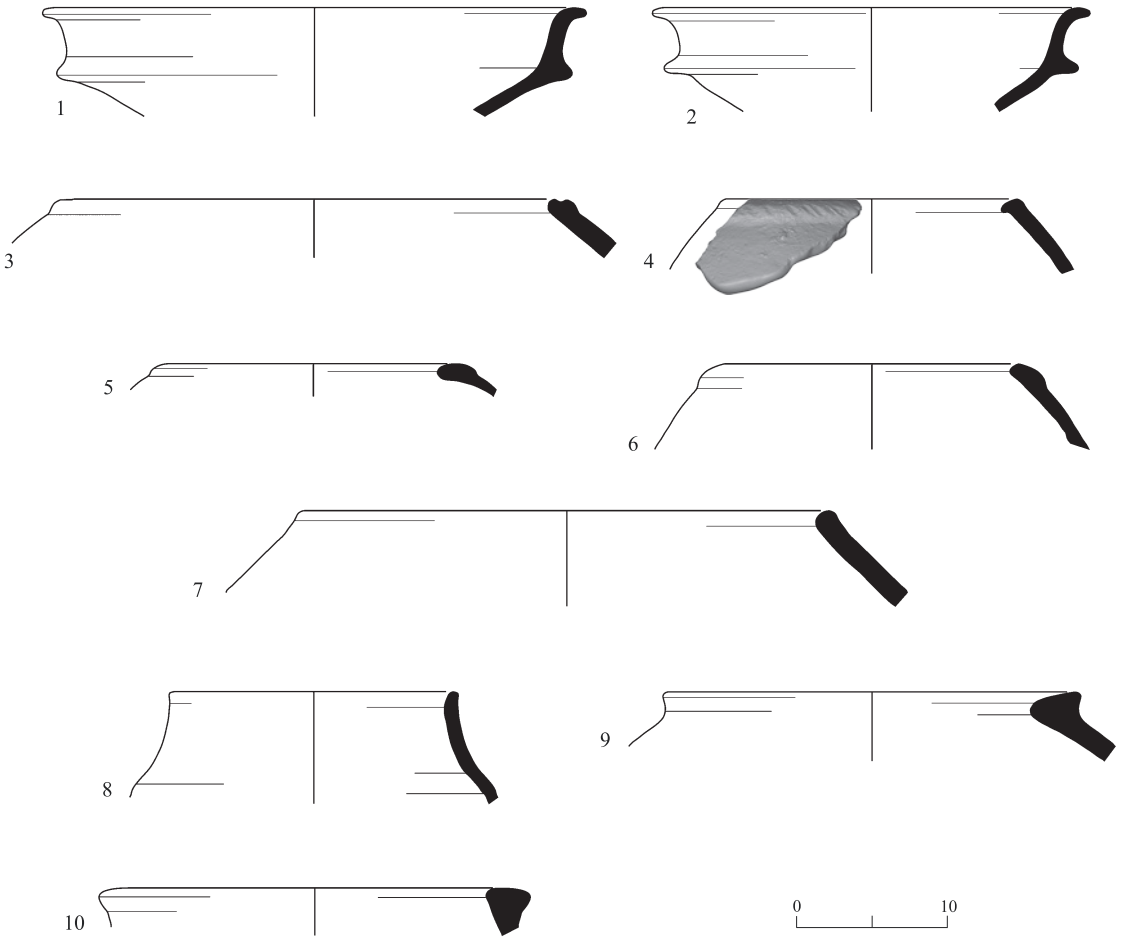

Fig. 4. Representative examples of EB IA pottery from ‘En Esur: GBW bowls (1, 2), holemouths (3–7) and jars/pithoi (8–10) (drawing: A. Gyerman-Levanon).

Eclipse 50i POL) in plane-polarized light (PPL) and cross-polarized light (XPL). Petrofabric descriptions follow standard nomenclature (Orton, Tyers and Vince 1993; Stoops 2003). The assessment of the petrofabrics focused on the clay matrix and the aplastic components of the sherds. The main objectives were to determine whether the raw material was available locally near each site and to explore similarities or differences in the production processes employed at each site.

Results

Upon microscopic inspection of the selected pottery sherds from Dor South and ‘En Esur, we identified eight distinct petrofabric groups: four from Dor South and four from ‘En Esur (Table 2). A macroscopic description of each group precedes the microscopic results.

Dor South Petrofabric Groups

Group A

The pottery samples in this group are of a light-brown color with visible white inclusions of about 2 mm in diameter (Fig. 5:a, b). This group is characterized by a highly calcareous matrix of light-brown color (in PPL) with abundant foraminifera microfossils, whose geological age we could not determine for lack of indicative foraminifera in the studied thin sections. The raw material of this group consists generally of marl. Subgroups were determined according to the aplastic components added to the paste during the pottery production process (Table 2).

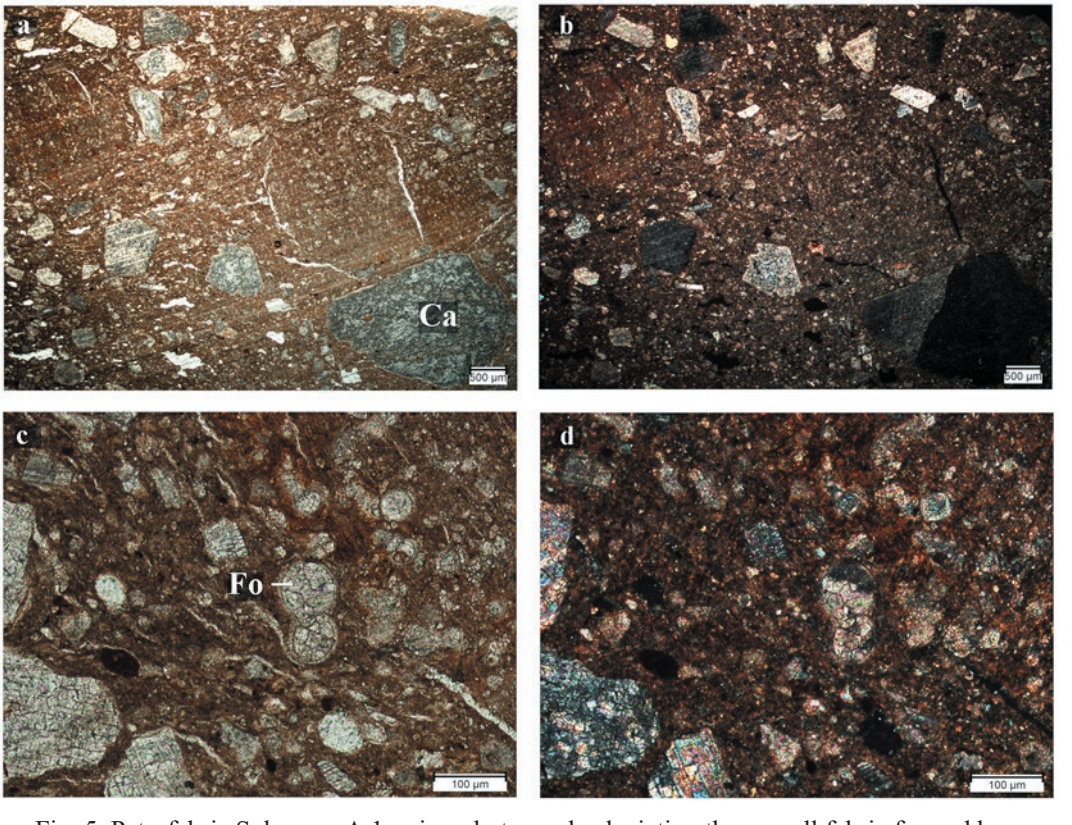

Fig. 5. Petrofabric Subgroup A.1: microphotographs depicting the overall fabric formed by a matrix of the calcareous marl formation with crushed sparitic calcite (Ca) inclusions in PPL (a) and XPL (b); higher magnification in PPL (c) and XPL (d) showing the abundance of foraminifera microfossils (Fo) in the paste.

Table 2. Petrographic Observations for Pottery from Dor South and 'En Esur.

Petrofabric Group/ Subgroup	N	Sample Nos.	Paste	% of Inclusions	Main Inclusions (% of Overall Inclusions)	Minor Inclusions (% of Overall Inclusions)	Voids	Comments
Dor South								
A.1	6	DS-1, 4, 6, 7, 9, 18	Light brown calcareous marl with abundant small microfossils (50%; diam. 50–100 µm)	30–40	Angular crushed sparitic calcite crystals (95%; diam. 300–2000 µm)	Grog and chalk (5%; diam. 300–500 µm); quartz silt (<1%; diam. 50–70 µm)	Elongated cracks; chamber voids (5%)	The main difference between these two subgroups is the size of the microfossils, possibly reflecting different source of material
A.2	2	DS-2, 8	Light brown calcareous marl with abundant large microfossils (50%; diam. 300 µm)	30–40	Angular crushed sparitic calcite crystals (95%; diam. 300–2000 µm)	Grog and chalk (5%; diam. 300–500 µm); quartz silt (<1%; diam. 50–70 µm)	Elongated cracks; chamber voids (5%)	
A.3.1	4	DS-5, 10, 14, 20	Light brown calcareous marl with abundant small microfossils (50%; diam. 50–100 µm)	25	Rounded to subrounded chalk (80%; diam. 250–2000 µm)	Subrounded to subangular quartz silt (20%; diam. 50–70 µm)	Elongated planar voids (10–20%)	
A.3.2	4	DS-11, 12, 13, 15	Light brown calcareous marl with abundant small microfossils (50%; diam. 50–100 µm)	5	Subrounded to subangular chalk and clay balls (100%; diam. 250 µm)	None	Chamber voids (<1%)	Inclusions are rare in this group
B	4	DS-16, 17, 19, 21	Reddish calcareous marl with abundant small microfossils (50%; diam. 50–100 µm); iron oxide granules (10%; diam. 40 µm)	30–40	Angular crushed sparitic calcite crystals (95%; diam. 300–2000 µm)	Subrounded quartz silt (<1%; diam. 20–50 µm)	Chamber voids (10%); elongated planar voids (<1%)	Ferruginous marl
C	2	DS-3, 23	Reddish-brown sandy loam	30–40	Subrounded to subangular quartz sand grains (95%; diam. 150–200 µm)	Mollusk shells and *kurkar* fragments (5%; diam. 3000 µm)	Planar voids (5%)	

Table 2. (cont.)

Petrofabric Group/ Subgroup	N	Sample Nos.	Paste	% of Inclusions	Main Inclusions (% of Overall Inclusions)	Minor Inclusions (% of Overall Inclusions)	Voids	Comments
D	1	DS-22	Dark red silty loam	50	Angular quartz silt–sand grains (50%; diam. 50–200 µm)	Elongated mica silt grains (1%; diam. 50 µm)	Elongated voids after chaff temper (50%; diam. up to 3000 µm)	Grass phytoliths occur within some of the elongated voids
'En Esur								
1	7	'En Esur-17.2, 17.3, 17.4, 17.6, 18.2, 18.4, 19.3	Brown calcareous marl with a few large microfossils (10–20%; diam. 250–500 µm); quartz silt (10–20%; diam. 50 µm); iron oxide granules (< 1%; diam. 50–300 µm)	30	Angular grog grains (50%; diam. 200–2000 µm); angular crushed sparitic calcite crystals (50%; diam. 200– 2000 µm)	Subrounded quartz sand grains (1%; diam. 100–200 µm)	Elongated cracks (10%)	
2	2	'En Esur-18.1, 19.1	Brown calcareous marl with a few small microfossils (20–30%; diam. 100–200 µm); quartz silt (10–20%; diam. 50 µm); iron oxide granules (< 1%; diam. 50–300 µm)	30	Angular grog grains (50%; diam. 200–2000 µm); angular crushed sparitic calcite crystals (50%; diam. 200– 2000 µm)	Subrounded quartz sand grains (1%; diam. 100–200 µm); angular basalt grains (1%; diam. 50–100 µm)	Elongated cracks (10%)	As opposed to Group 1, this group includes more microfossils, though smaller in size, and basalt grains
3	2	'En Esur-17.5, 18.5	Brown calcareous marl and reddish silty loam; quartz silt (30%; diam. 20–60 µm)	40–50	Angular crushed sparitic calcite crystals (60%; diam. 300–2000 µm); grog grains (35%; diam. 0.5–3.0 mm)	Rounded quartz sand grains (5%; diam. 200 µm)	Elongated cracks (10%)	The quartz probably originated in *ḥamra* soil
4	1	'En Esur-19.2	Yellowish calcareous marl with very few microfossils (5%; diam. 200 µm); quartz silt (10–20%; diam. 20–60 µm)	35	Rounded quartz sand grains (84%; diam. 200 µm)	Angular chalk grains (14%; diam. 200 µm); angular sparitic calcite crystals (1%; diam. 200 µm); angular basalt sand grains (1%; diam. 200 µm)	Chamber voids (<5%)	Ferruginous microfossils

Subgroup A.1. The matrix consists of a calcareous clay with an abundance of microfossils ranging in sizes from silt to very fine sand (the largest with a diam. of 100 µm; Fig. 5:c, d). Under XPL the matrix is optically inactive. The aplastic inclusions comprise about 30–40% of the thin section area and consist predominantly of crushed angular sparitic calcite grains, which were intentionally added and range in size from fine to very coarse sand (the largest fragment measuring 2 mm in diam.; Fig. 5: a, b). In addition, there are a few grains of grog (crushed pottery) and rounded grains of foraminiferous chalk. Quartz grains are rare (<1%) and are silt- to very fine sand-sized (diam. 50–70 µm). Elongated cracks occur near the inclusions, possibly from shrinkage, while chamber voids may indicate evaporation of water from the paste during the pottery drying/firing process (Fig. 5; Table 2). Two samples in this subgroup (DS-7 and DS-9) differ slightly from the rest, with a more densely packed matrix, fewer (10–20%) and smaller (mostly with diam. ≤250 µm) sand-sized aplastic components of crushed sparitic calcite and fragments of chalk.

Subgroup A.2. This subgroup is similar to Subgroup A.1 in the matrix and aplastic inclusions but differs from it in the size of the microfossils (Fig. 6). The foraminifera present in the paste of this subgroup are larger (diam. 300 µm; Fig. 6:b). The rationale for placing these in a separate subgroup is that larger microfossils may indicate sea conditions different from those where smaller microfossils were found, possibly indicating that raw material was quarried from a different marl exposure than that of Subgroup A.1.

Subgroup A.3. This subgroup comprises a matrix similar to that of other Group A subgroups—that is, predominantly marl—however, it does not contain crushed sparitic

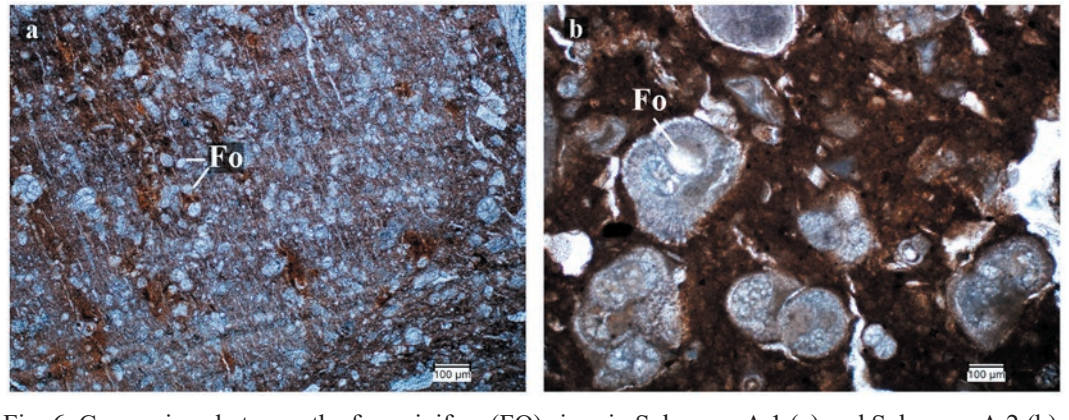

Fig. 6. Comparison between the foraminifera (FO) sizes in Subgroup A.1 (a) and Subgroup A.2 (b) at the same magnification.

calcite inclusions. It is further subdivided into two groups, based on the type of aplastic inclusions. In Subgroup A.3.1, 25% of the thin section area is composed of inclusions, 80% of which are rounded to subrounded chalk fragments ranging in sizes from medium sand to very coarse sand (250–2000 µm; Fig. 7:b, c), and the other 20%, subrounded to subangular silt- to very fine sand-sized quartz grains (50–70 µm) (Fig. 7:a). The aplastic inclusions in Subgroup A.3.2 comprise only <5% of the thin section area, composed of fine sand-sized to medium sand-sized (up to 250 µm) subrounded to subangular chalk grains and clay balls (Fig. 8:a, b; Table 2). No quartz grains are visible in this group. The occurrence of silt- to sand-sized quartz grains in Subgroup A.3.1 suggests that the paste was derived from soil, likely rendzina, which may have developed from marl.

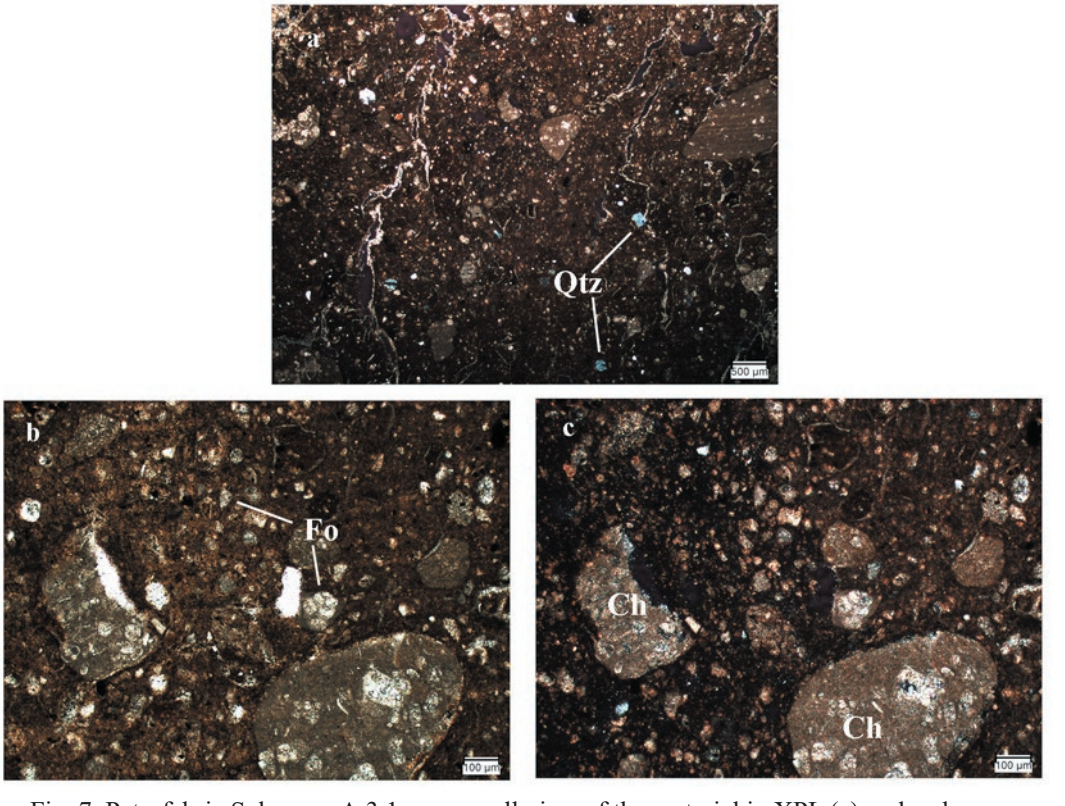

Fig. 7. Petrofabric Subgroup A.3.1: an overall view of the material in XPL (a) and a close-up in PPL (b) and XPL (c); the majority of aplastic inclusions in this group are rounded grains of foraminiferous chalk (Ch); some silt-sized quartz grains (Qtz) are present in this fabric, as well as foraminifera microfossils (Fo).

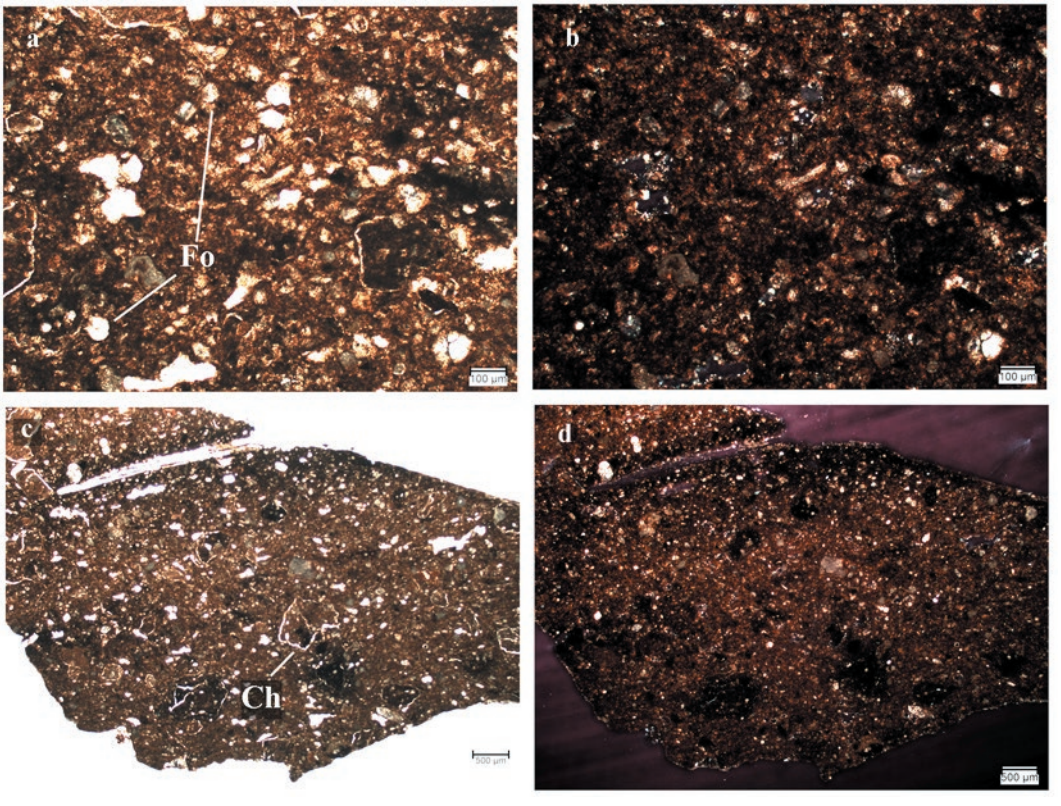

Fig. 8. Petrofabric Group A.3.2: close-up of the matrix in PPL (a) and XPL (b), and an overview of the slide showing the inclusions in PPL (c) and XPL (d); the homogenous matrix in this group contains small-sized foraminifera (Fo), similar to Subgroups A.1 and A.2 (a), and few aplastic inclusions of rounded grains of foraminiferous chalk (Ch) (c).

Group B

The pottery samples in this group are of a reddish color, with visible white inclusions measuring about 2 mm in diameter. This group is very similar to Group A, with a calcareous matrix and crushed sparitic calcite inclusions; however, the reddish color (in PPL) of the matrix sets it apart (Fig. 9:a, b), possibly indicating a different origin of the paste material. The matrix comprises dense foraminiferous marl with silt-sized (diam. ≤40 µm) rounded granules of iron oxides (5–10%). Abundant foraminifera are present, some of which are stained by the ferric oxides (Fig. 9:c, d), as well as sea urchin spines, which were not identified in the other petrofabric groups (Fig. 9:a). Under XPL the fabric is optically inactive. Aplastic inclusions comprise 30–40% of the thin section area; they are predominantly of crushed angular sparitic calcite ranging in sizes from fine to very coarse sand (as large as 2 mm), and some have a gray tint, perhaps indicating high firing temperatures (Fig. 9:a). Other visible aplastic components are occasional (<1%) subrounded silt- to very fine sand-sized quartz grains (diam. 20–50 µm). The voids make up about 10% of the thin section area and are mainly chamber voids with occasional

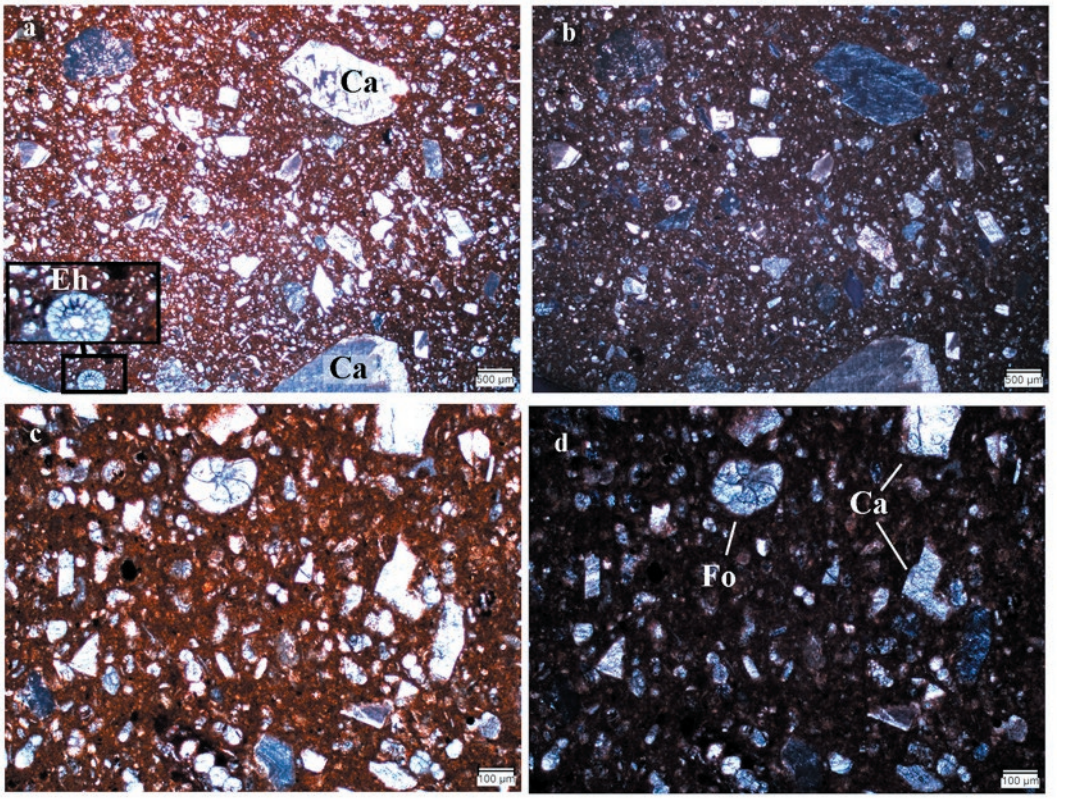

Fig. 9. Petrofabric Group B: an overall view of the material in PPL (a) and XPL (b) and a close-up in PPL (c) and XPL (d); the matrix is reddish with foraminifera microfossils (Fo) (c, d) and sea urchin spines (Eh) (a), most aplastic inclusions are crushed sparitic calcite crystals (Ca) (a).

(<1%) elongated planar voids similar to those present in Subgroup A.1 (Table 2). The matrix of this group is also identified as marl.

Group C

The pottery samples in this group are reddish brown with a gritty texture. Most of the inclusions are not visible to the naked eye, with the exception of a few fragments measuring about 2 mm in diameter. The matrix is of a reddish (in PPL) silty loam that is optically inactive (in XPL). The voids are mainly very thin planar voids (5%), which may represent shrinkage and cracking during the drying and/or firing processes. Aplastic inclusions are mainly subrounded to subangular quartz grains of fine-sand size (diam. 150–200 µm), and they represent 30–40% of the thin section area (Fig. 10). In addition, there are some shell fragments (Fig. 10:c), as well as fragments of *kurkar* (Fig. 10:a; Table 2). This matrix and the aplastic inclusions of this group suggest a provenance in the coastal area (Waiman-Barak, Gilboa and Goren 2014:329–330; Ogloblin Ramirez, Galili and Shahack-Gross 2021:121).

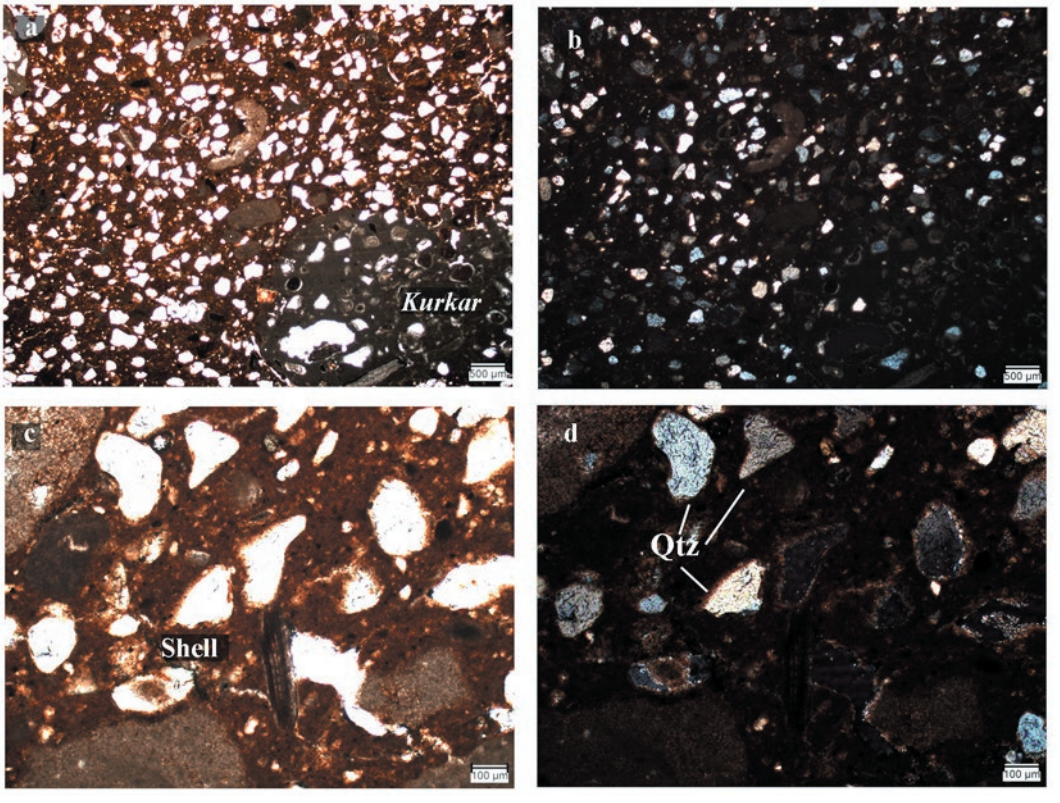

Fig. 10. Petrofabric Group C: an overall view of the material in PPL (a) and XPL (b), and a close-up in PPL (c) and XPL (d); this group is characterized by the abundance of quartz sand grains (Qtz) (a, d) and includes *kurkar* inclusions (a) as well as mollusk shell fragments (c).

Group D

One pottery sample belongs to this group. It is dark red with a gritty texture. The matrix is a dark red (in PPL) silty loam that is optically inactive (in XPL). Many elongated voids (30%), some up to 3 mm long, are visible and seem to be pseudomorphic after chaff temper. This identification is supported by the presence of elongated grass phytoliths within some of these voids (Fig. 11:c). Aplastic inclusions comprise about 50% of the sample; about half of them are the voids of chaff temper, and the other half are quartz grains of varying sizes, mostly very fine sand-sized (diam. c. 50 µm), with few reaching the upper limit of fine sand-size (diam. 200 µm; Fig. 11:b). The quartz grains in this sample are mostly angular with some reaching subrounded shapes, indicating that the material had not traveled far from its origin (Fig. 11:d). In addition, elongated (diam. 50 µm) mica laths are present in the matrix (Fig. 11:d). The presence of fine sand-sized angular quartz grains together with mica suggests an origin in Nile sediments (Waiman-Barak, Gilboa and Goren 2014:326–330).

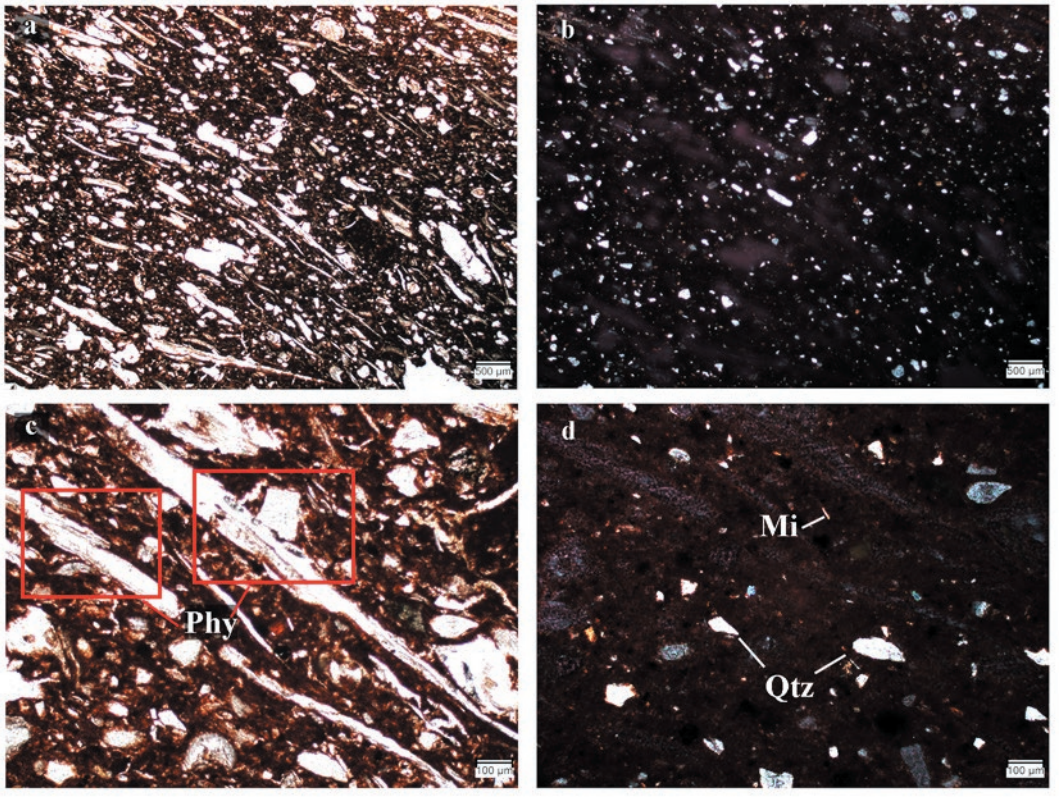

Fig. 11. Petrofabric Group D: an overall view in PPL (a) and XPL (b,) and a close-up in PPL (c) and XPL (d); most aplastic inclusions in this group are silt to sand-sized quartz grains (Qtz) in addition to some mica grains (Mi) (d); grass phytoliths (Phy) occur within the elongated voids indicating they originate in chaff temper (c).

Overall, two petrofabric groups identified at Dor South are based on a marl paste, a third group is based on eastern Mediterranean coastal sediments, and a fourth, on Nile sediments.

‘En Esur Petrofabric Groups

Group 1

The pottery samples in this group are light brown, with visible grog inclusions measuring about 2 mm in diameter (Fig. 12:a, b). This group is characterized by matrix features similar to those of Dor South Group A, i.e. dominated by marl.

The matrix consists of brown calcareous and slightly foraminiferous marl containing quartz silt (10–20%; diam. c. 50 µm) and fine sand-sized (<1%; diam. 50–300 µm) granules of iron oxide. The identifiable foraminifera include Paleogene *Globigerinoides* (Fig. 12:c) and apparent Upper Cretaceous *Lenticulina* (Fig. 12:d) and *Heterohelix*. Elongated/hairline cracks occur near the inclusions (10%) and may be the result of shrinkage during the pottery

drying/firing process. Sand-sized aplastic inclusions comprise approximately 30% of the sample and consist predominantly of angular grog fragments (Fig. 12:a) and crushed sparitic calcite grains ranging in sizes from medium to coarse sand (diam. 0.2–2.0 mm; Fig. 12:c). In addition to the two main inclusions stated above, there are very fine to fine sand-sized subrounded quartz grains (diam. 100–200 µm; Fig. 12:c).

The presence of Paleogene and Upper Cretaceous foraminifera, along with the abundance of silt-sized quartz grains, strongly suggests that the raw material originated in soil or alluvium that developed from marl. This proposition aligns with the characteristics observed in sediments collected by the ‘En Esur petrography research team (current authors A.S., A.C.-W., I.E. and Y.P.) during a survey conducted around the ‘En Esur site.

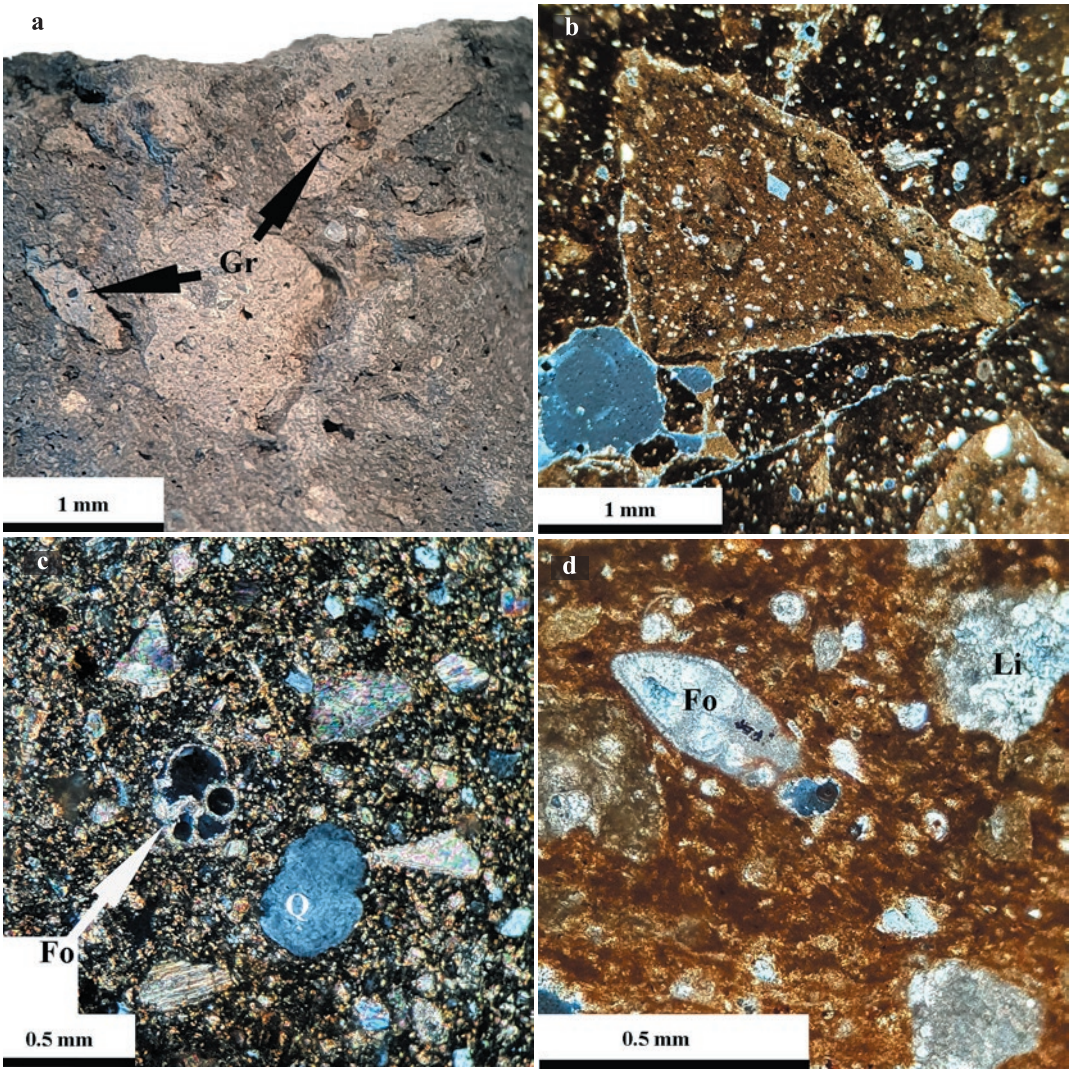

Fig. 12. Petrofabric Group 1: an overall view of the material in PPL (a) and XPL (b), and a close-up in PPL (c) and XPL (d); the matrix is light brown with foraminifera microfossils (Fo) (c, d); the aplastic inclusions are mostly crushed pottery (grog; Gr) (a).

Group 2

The matrix, otherwise similar to that of Group 1, differs from it by the higher percentage of microfossils (20–30%) and their smaller, mostly fine sand-size (the largest measuring 200 µm in diam.; Fig. 13:a, c). In addition, a difference in the morphotypes of these microfossils was documented with the identification of Echinoidea spines (Fig. 13:a). Elongated cracks appear, similarly to those in Group 1, near the inclusions (10%). The aplastic inclusions in this group are, for the most part, like those in Group 1, with grog and crushed sparitic calcite grains, as well as occasional quartz grains. The difference from Group 1 is the presence

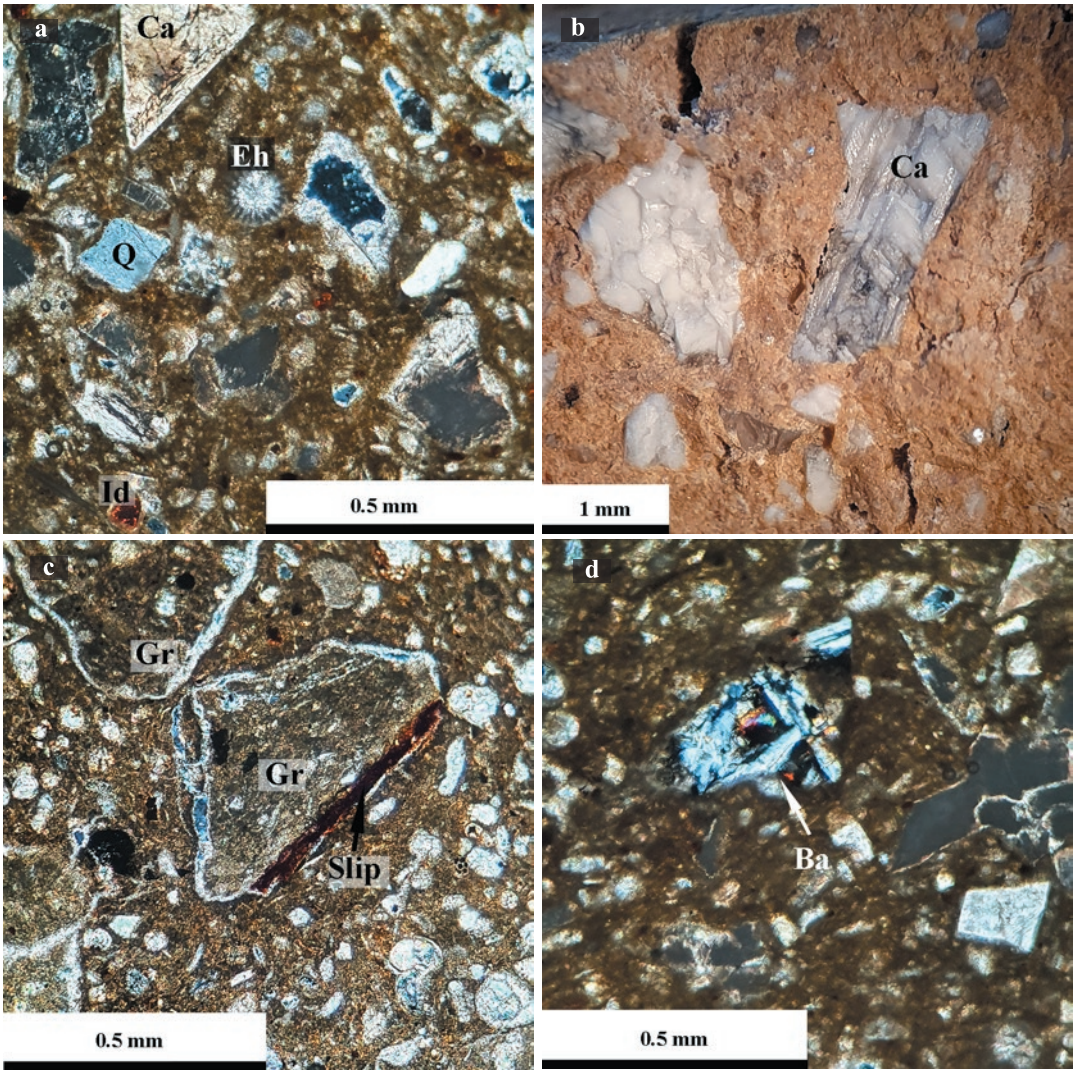

Fig. 13. Petrofabric Group 2: an overall view of the material in XPL (a) and PPL (b); the matrix is light brown with foraminifera microfossils (Fo) and sea urchin spines (Eh) (a, c); the aplastic inclusions are mostly crushed sparitic calcite (Ca) and crushed pottery (grog; Gr) (a, c), with occasional quartz grains (Q) (a) and basalt (Ba) (d).

of occasional (1%) silt- to very fine sand-sized (diam. 5–100 µm; Fig. 13:a, b, c) basalt fragments (Fig. 13:d). The raw material of this group seems to be predominantly marl.

Group 3

The pottery samples in this group are light brown to reddish in color with visible white inclusions of about 2 mm in diameter (Fig. 14:a, b). The matrix is light brown to reddish color (in PPL) and optically inactive (in XPL). Aplastic inclusions comprise 40–50% of the thin section area, with crushed angular sparitic calcite (as large as 2 mm) accounting for 50%, grog (as large as 3 mm) accounting for 35%, and silt- and fine sand-sized (diam. ≤200 µm) quartz grains accounting for 15% (Fig. 14:b–d). Elongated cracks are visible

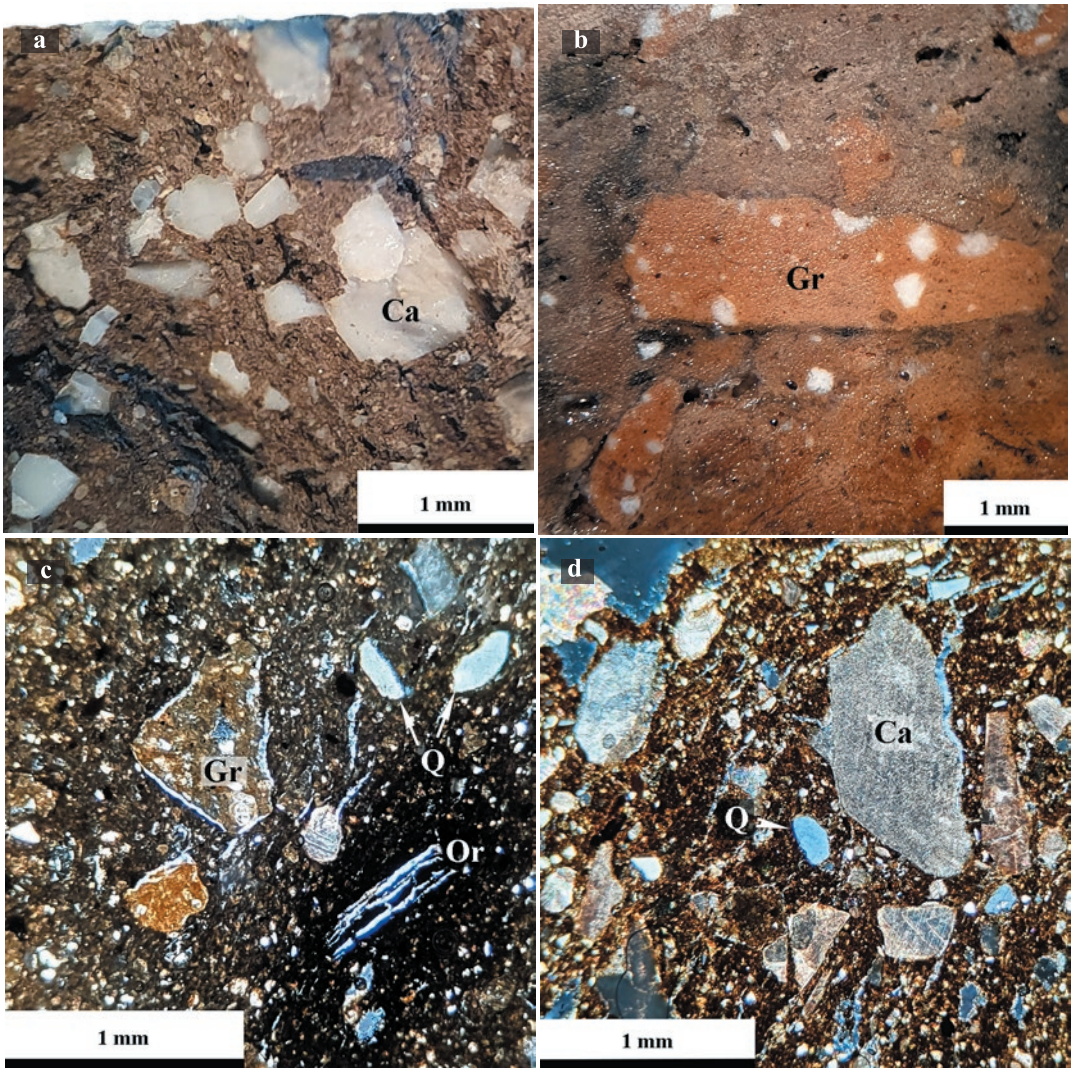

Fig. 14. Petrofabric Group 3: an overall view of the material in PPL (a, b); the matrix is light brown and includes some silt-sized quartz grains; the aplastic inclusions are mostly crushed sparitic calcite (Ca) and crushed pottery (grog; Gr) (a–d) in addition to quartz grains (Q) (c, d).

(10%) near the inclusions, similar to those in Groups 1 and 2. The red color of this group in comparison with Group 1 suggests the paste is a mixture of marl and a local ferruginous sandy soil, *ḥamra* (possibly after sieving some of the larger sand-sized grains).

Group 4

The pottery sample in this group is of a yellowish color with small clear inclusions up to 0.5 mm in diameter (Fig. 15). The matrix consists of a yellowish (in PPL) calcareous clay (i.e., marl) and is optically inactive (in XPL), containing a small number of fine sand-sized foraminifera microfossils (c. 5%) and quartz silt (diam. 20–60 µm) representing approximately 10% of the matrix. Some of the microfossils have an iron oxide infilling/

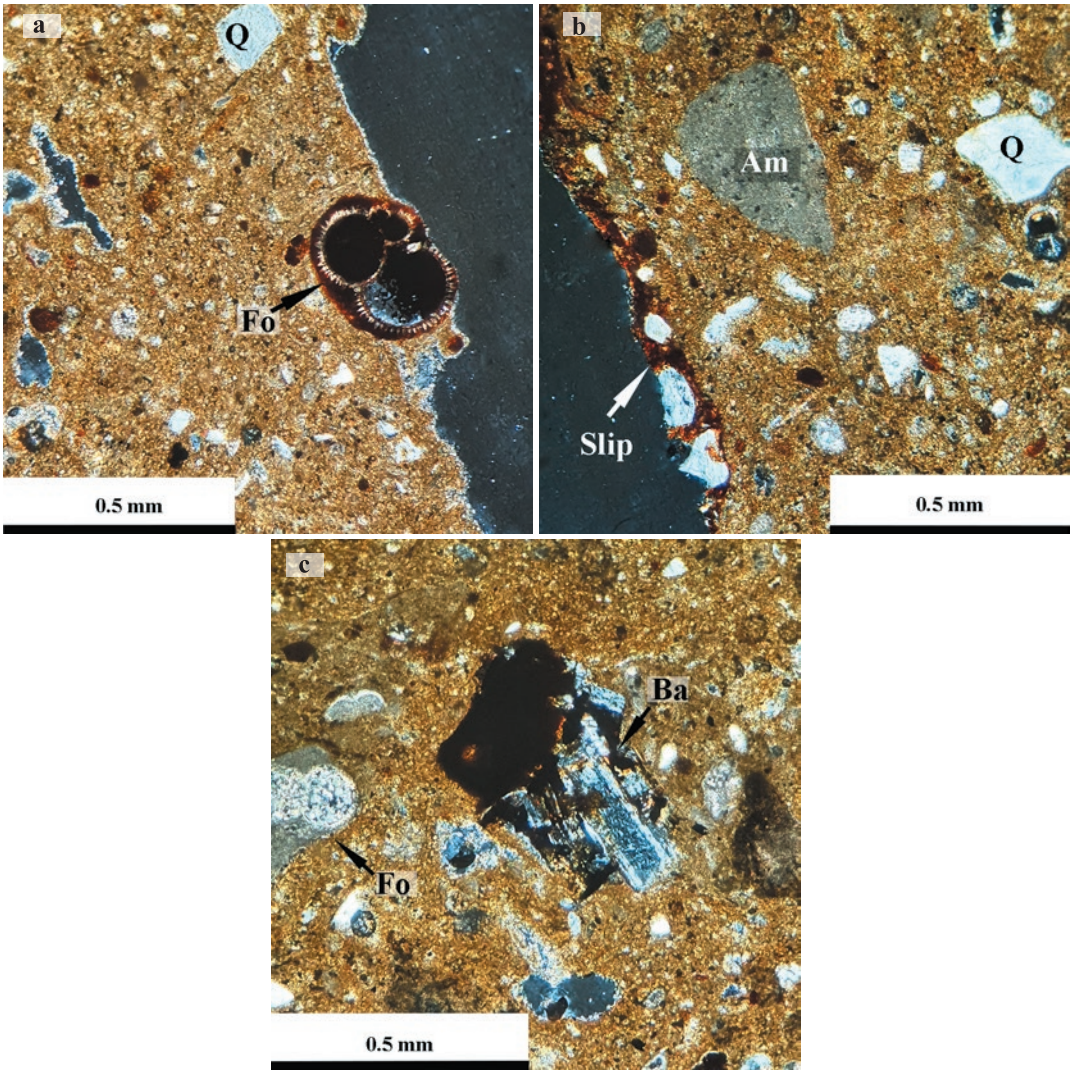

Fig. 15. Petrofabric Group 4: an overall view of the material in XPL (a, b); the matrix is yellowish with foraminifera microfossils (Fo), some with iron oxide filling (a); the aplastic inclusions are mostly rounded quartz grains (Q) (a, b), with the addition of rare presence of possible *Amphiroa* sp. algae (Am) (b) and basalt grains (Ba) (c).

coating (Fig. 15:a), and iron oxide specks are visible throughout the matrix. Aplastic components represent 35% of the thin section area and consist mainly of fine sand-sized rounded quartz grains (diam. 200–500 µm; Fig. 15:b), representing about 85% of the inclusions, as well as some grains of foraminiferal chalk (c. 15%) of the same size. Other, rare, aplastic components are a possible *Amphiroa* sp. algae fragment (Fig. 1:5b), crushed sparitic calcite grains (1%; diam. 200 µm) and eroded basalt grains (1%; diam. 500 µm; Fig. 15:c).

Overall, at ‘En Esur all four petrofabric groups seem to be based on a marl paste that was sometimes mixed with soil or alluvial deposits. The characteristics of Group 4 may suggest an origin in the Chekka Formation marl, which occurs along the coast of Lebanon. However, it is important to note that as the latter is not easily distinguishable from the Taqiye Formation, we cannot establish this connection securely.

Discussion

Four major petrofabric groups were identified at Dor South and four at ‘En Esur (Table 3). The results indicate a notable prevalence of non-coastal material within the Dor South assemblage, in contrast to ‘En Esur, where locally available resources appear to have been the most commonly used materials. These similarities and differences shed light on certain aspects of the economic structure at each of the studied sites.

Similarities and Differences among the Petrofabric Groups

At both ‘En Esur and Dor South the data indicate that marl (whether Cretaceous or Paleogene), or soil derived from marl, is the dominant raw material chosen for pottery production, and that crushed sparitic calcite was a preferred aplastic inclusion in EB IA (petrofabric Groups A, 1, 2). Ferruginous marl is also present at both sites (petrofabric Groups B, 4), but was

Table 3. Summary of Petrofabric Groups Identified at Dor South and ‘En Esur and Their Proposed Origin

Site	Petrofabric Group	No. of Samples	Proposed Origin
Dor South	A	N = 16	Unknown (not coastal)
Dor South	B	N = 4	Unknown (not coastal)
Dor South	C	N = 2	Israeli coast
Dor South	D	N = 1	Egypt
‘En Esur	1	N = 7	Local, close to site
‘En Esur	2	N = 2	Local, close to site
‘En Esur	3	N = 2	Local, close to site
‘En Esur	4	N = 1	Lebanon coast

probably of different origins, as Dor South Group B includes abundant grains of crushed sparitic calcite and lacks appreciable amounts of quartz, while ‘En Esur Group 4 contains rare grains of crushed sparitic calcite and abundant fine sand-sized quartz grains. The latter likely originated in the Senonian–Paleogene Chekka Formation in Lebanon (Bellos 2008:59–62), indicating a possible import to ‘En Esur. A clear import at Dor South is a vessel with petrofabric characteristics of Egyptian raw materials (Waiman-Barak, Gilboa and Goren 2014:326–330). Both sites yielded also pottery of a petrofabric abundant with quartz sand—Group C at Dor South and Group 3 at ‘En Esur—yet their origins seem to differ, with Group C having clear coastal components and Group 3 showing a mixture of marl with a local sandy soil (*ḥamra*).

As stated above, Dor South Group A and ‘En Esur Group 1 are alike in their matrix and major aplastic inclusions. However, the presence of silt- and fine sand-sized quartz grains in ‘En Esur Group 1 (10–20% of the ceramic matrix) and their near absence from Dor South Groups A and B (0–5% of the ceramic matrix) reveal that these groups are inherently different and could not have been produced from the same source material. This assertion is further supported by the higher variability of aplastic components in ‘En Esur Group 1 (including crushed sparitic calcite, quartz, basalt and grog) versus Dor South Groups A and B, which mostly incorporate either sparitic calcite or chalk fragments. Overall, it appears that each site has its unique petrofabric assemblage, indicating different origins of paste raw materials, as well as certain international connections (see below).

The Economic Systems of Dor South and ‘En Esur Based on the Ceramic Petrography

Although pottery is not the main component of village economies, it provides key insights into choices made by ancient populations. The differences between the sites’ petrofabric groups show that ‘En Esur and Dor South were engaged in different economic systems that involved pottery production and trade. It is therefore imperative that each system be examined through the available raw materials around the settlements to determine the extent of local production and trade at each site.

At ‘En Esur, most of the pottery (11 of 12 samples) appears to have been locally produced. This is inferred from the presence of marl outcrops (primarily the Taqiye Formation) to the east of the site, and *ḥamra* next to the site, to its west, but also below it, as the site was founded opon it. The quartz component commonly visible in petrofabric Groups 1, 2 and 3 originated either in *ḥamra* soil or in dust incorporated into the surface of (most probably) Taqiye marl outcrops or soil that developed on them in a process of pedogenesis. The most common aplastic components, sparitic calcite and grog, can also be sourced locally: calcite, from veins within dolomite, chalk and limestone rocks—which occur in the vicinity of the site (Sneh et al. 1996)—and grog, from crushed pottery, which would have been available in a pottery production site. The occasional basalt grains identified in the pottery of ‘En Esur probably originated in eroded basalt outcrops that occur approximately 6 km east of the site (Sneh et al. 1996), and were likely transported along the westward-flowing Naḥal ‘Iron, which runs close to the site. Group 4 is the only one that is suspected to have been imported

to the site, possibly deriving from the Chekka Formation in Lebanon (Walley 1997). With a single representative at ‘En Esur among dozens of sherds, this group stands out also in its small size, suggesting a potentially non-local origin amid an assemblage of predominantly locally produced pottery.

The situation at Dor South is completely different. Most of the pottery (21 of 23 samples) seems to have been imported to the site. The most common petrofabric Group A was produced from raw material that is not locally available, as marl does not occur on the coast, and farther east—on Mount Carmel—there are no known marl formations (Segev and Sass 2009). The nearest outcrop of marl, of the Taqiye Formation, is more than 10 km away from the site (Segev and Sass 2009; Ogloblin Ramirez et al. 2021). The near absence of quartz silt- or sand-sized grains in Group A further supports this notion, as even if the raw material had been brought from afar and manipulated at this coastal site, quartz grains would have been present, indicating that complete vessels were imported to the site. The other two groups representing imports, Groups B and D, hint at the extent of the trade networks active along the coast, both to the north and to the south of Dor South. As stated above, Group B bears similarities to the possibly Chekka marl Group 4 from ‘En Esur, with the ferruginous rich material and infill of microfossils; however, it differs from it substantially by containing abundant crushed sparitic calcite grains and lacking quartz grains and basalt fragments. A single sherd with a petrofabric typical of Nile sediments supplies the only indication of the presence at the site of Egyptian-made pottery, pointing to potential connections between Dor South and Egypt. This is inferred from the micaceous nature of the paste raw material, which occurs commonly in Nile sediments (e.g., Waiman-Barak, Gilboa and Goren 2014:326–330). It also differs from all other petrofabrics at both Dor South and ‘En Esur in evidence of chaff temper.

Egyptian pottery or influences are not known in EB IA contexts in Israel, and first appear only in EB IB, mostly in southern and central Israel, in coastal sites such as Palmaḥim and Lod (see, e.g., Miroschedji 2002; Braun 2014; Paz 2023). An Egyptian vessel found in the sea near ‘Atlit, though it is a single piece of evidence, indicates possible maritime connections between Egypt and the northern coast during EB IB (Sharvit et al. 2002).

Lastly, the only petrofabric group at Dor South that may be identified as produced on the coast is Group C. The fine sand-sized quartz grains, *kurkar* and shell grains are commonly regarded as indicators of coastal production (Waiman-Barak, Gilboa and Goren 2014:329–330; Ogloblin Ramirez, Galili and Shahack-Gross 2021:121). A comparison of the size and roundness of the quartz grains in this group, with control samples from the Newe Yam region (Ogloblin Ramirez et al. 2021:134), suggests that the two sherds belonging to Group C were produced locally. Importantly, the ratio of these sherds, along with the Egyptian sherd, to the remaining twenty items in the sample assemblage does not represent the percentage of vessels from these petrofabric groups in the site’s assemblage, as they were selected for analysis intentionally, based on their unique macroscopic features, rather than randomly, like the rest of the samples. The limited, perhaps only sherds of this kind among the site’s excavated assemblage indicate that coastal pottery, as well as Egyptian imports, were rare

at Dor South. The results present two main economic choices that were made by the sites' inhabitants: (1) a change in resource management; or (2) an interaction between the sites and trade engagements.

(1) A Change in Resource Management. At ʻEn Esur, pottery was locally produced with some imports, indicating a diversity of ceramic resources, which contributed to societal resilience. Moreover, the standardized pottery wares on the one hand, and the rather limited petrofabric groups on the other, attest to the beginning of craft specialization at the site. It is evident that ʻEn Esur was showing first signs of an urban economy as early as EB IA, as two of the main characteristics of urban economy—craft specialization and command over local resources—are reflected in the studied pottery assemblage. This may have eventually contributed to the growth of the EB IB city at ʻEn Esur, which boasted public structures and other monumental architecture, and was engaged in local and long-distance trade, attested by non-local materials, such as basalt objects, and Egyptian goods found in mortuary contexts at the site (Paz, Elad and Cohen-Weinberger 2021). Dor South, on the other hand, consumed primarily pottery that was produced inland, where marl was utilized (possibly from the Taqiye Formation, the nearest marl source, in the Menashe Hills to the east), and engaged only marginally in the production of (low quality, coastal) pottery. Overall, the site conducted a nondiversified ceramic economy that focused on acquiring pottery by trade—overland or maritime—putting its population at risk of being dependent on other settlements and increasing its fragility in times of changes that were beyond its control. It is noteworthy that the investment in imported pottery was not due to lack of clay resources on the Carmel Coast but rather a conscious choice.

From a temporal point of view, Dor South is currently the only pottery-bearing site in the Carmel Coast that did not rely on local pottery production. Neolithic and Chalcolithic sites, such as Ha-Bonim North, Newe Yam and Tell Ḥreiz, which produced pottery from locally sourced materials, are good examples of the developing stable coastal village system in the region (Ogloblin Ramirez et al. 2021; Nickelsberg et al. 2024). Later coastal settlements also produced pottery from local materials (Waiman-Barak, Gilboa and Goren 2014; Ratzlaff et al. 2017). From a regional point of view, a comparison between EB IA pottery production dynamics at different coastal settlements in Israel shows slight differences between the southern coastal plain and Dor South, though there are some similar trends. At Ashqelon, Barneʻa, for example, local pottery production continued, as in previous periods; however, local wares comprise only around 50% of the petrographic samples from the site and are supplemented with multiple other petrofabric groups that arrived at the site through trade (Cohen-Weinberger 2022: Table 2.1). The amount of imported pottery is significantly larger at these two coastal sites than at ʻEn Esur, as demonstrated by the samples from the latter.

(2) Interaction between the Sites and Trade Engagement. Although we would have expected ʻEn Esur and Dor South to have interacted, due to the visible similarities in the pottery

assemblages and the short distance between them, this does not seem to be the case. The clay recipes found at both sites are different, indicating that pottery was not exchanged/traded between them. This does not mean that Dor South was not connected with other inland settlements, as is evident from the presence at the site of basalt groundstones and flint items from various sources (Shahack-Gross et al. 2024), yet it may have not been connected with rising powers that could have contributed to its resilience. Furthermore, we note that there are similarities between petrofabric Groups A and B of Dor South and Group B of Ashqelon, Barne‘a (see Cohen-Weinberger 2022:95–96), suggesting a coastal economic trade system encompassing the northern and southern coastal EB IA sites, which was only loosely connected to major inland sites.

The observations presented above show that coastal EB IA communities made at least two economy-related decisions that may have led to their demise. First, they reduced the use of local clay for pottery production, which had been a part of the coastal economy for thousands of years, consequently becoming more dependent on traded pottery. The lack of diversification of ceramic resources may have reduced the resilience of these communities to changes in trade networks. Second, they seem to have been engaged in various trade networks but perhaps not with those that could have offered support in the face of societal decline/collapse. While these ideas are based on relatively small data sets, they may serve as a basis for future detailed research.

Conclusions

The petrographic analyses conducted on pottery from the inland site of ‘En Esur and the coastal site of Dor South show that each had elected a significantly different strategy of pottery production and trade. While the ‘En Esur inhabitants chose to focus on local production, the Dor South residents relied mainly on trade. The path chosen by Dor South, and possibly by other sites that were engaged in the same economic system, preferring dependence on trade networks and low diversification of ceramic resources, appears to have jeopardized the resilience of these coastal communities, and may even be viewed as one of the reasons for the eventual abandonment of the coast by the end of EB I.

The results and possible interpretations presented above set the groundwork for future research of the coastal village system of EB IA through an examination of the use of local versus distant resources, such as pottery, mud bricks and building stones. Such studies may provide new data to explain the abandonment of the coastal environment at a time in which this region would have been expected to thrive and support the growing urban economy.

Acknowledgements

We thank the Leon Recanati Institute for Maritime Studies and the Department of Maritime Civilizations at the University of Haifa, without whom the excavation at Dor South could

not have succeeded. Brigid Clark, Sára Lantos, Sara Macke and Alyssa Pietraszek assisted in the excavations and post-excavation processing. We would also like to thank Jonathan J. Gottlieb for the preparation of the Dor South petrographic thin sections and Paula Waiman-Barak for assisting in the initial thin section observations.

Funding Statement

This research was funded by the Israel Science Foundation (Grant no. 697/20 to Ruth Shahack-Gross). Roey Nickelsberg was supported by a Haifa Center for Mediterranean History Ph.D. Scholarship, the Nathan Rotenstreich Scholarship for outstanding Ph.D. students in the humanities and the Sir Maurice and Lady Irene Hatter Research Grant from RIMS.

References

Adams M.J., David J., Homsher R.S. and Cohen M.E. 2014. The Rise of a Complex Society: New Evidence from Tel Megiddo East in the Late Fourth Millennium. *NEA* 77:32–43. https://doi.org/10.5615/neareastarch.77.1.0032

Bellos G.S. 2008. *Sedimentology and Diagenesis of Some Neocomian-Barremian Rocks (Chouf Formation), Southern Lebanon*. M.A. thesis. American University of Beirut. Beirut.

Braun E. 2014. Observations on Contacts between the Nile Valley and the Southern Levant in Late Prehistory Prior to Dynasty 0. In M.A. Jucha, J. Dębowska-Ludwin and P. Kolodziejczyk eds. *Aegyptus est imago caeli: Studies Presented to Krzysztof M. Cialowicz on His 60th Birthday* (Publication of the Institute of Archaeology, Jagiellonian University). Kraków. Pp. 223–234.

Chesson M.S. 2019. The Southern Levant during the Early Bronze Age I–III. In A. Yasur-Landau, E.H. Cline and Y.M. Rowan eds. *The Social Archaeology of the Levant from Prehistory to the Present*. Cambridge–New York. Pp. 163–182. https://doi.org/10.1017/9781316661468.011

Cohen-Weinberger A. 2022. Petrographic Analysis of Selected Vessels. In A. Golani. *Ashqelon Barne'a; The Early Bronze Age Site* II: *The Finds* (IAA Reports 70). Jerusalem. Pp. 91–99.

Dan J., Raz Z., Yaalon D.H. and Koyumdjisky H. 1975. *Soil Map of Israel.* Tel Aviv.

Elad I. and Paz Y. 2018. 'En Esur (Asawir). *HA–ESI* 130 (July 16). http://www.hadashot-esi.org.il/report_detail_eng.aspx?id=25453&mag_id=126 (accessed May 12, 2024).

Elad I. and Paz Y. 2023. 'En Esur: An EBIB Urban Center at the Coastal Plain of Israel and Its Role in the Early Urbanization of the Southern Levant. In N. Marchetti, F. Cavaliere, E. Cirelli, C. D'Orazio, G. Giacosa, M. Guidetti and E. Mariani eds. *Proceedings of the 12th ICAANE Congress on the Archaeology of the Ancient Near East, 06–09 April 2021, Bologna* 2: *Field Reports; Islamic Archaeology.* Wiesbaden. Pp. 203–216. https://doi.org/10.13173/9783447119030.203

Faust A. and Ashkenazy Y. 2009. Settlement Fluctuations and Environmental Changes in Israel's Coastal Plain during the Early Bronze Age. *Levant* 41:19–39. https://doi.org/10.1179/175638009x448230

Frechen M., Neber A., Tsatskin A., Boenigk W. and Ronen A. 2004. Chronology of Pleistocene Sedimentary Cycles in the Carmel Coastal Plain of Israel. *Quaternary International* 121/1:41–52. https://doi.org/10.1016/j.quaint.2004.01.022

Gophna R. and Portugali J. 1988. Settlement and Demographic Processes in Israel's Coastal Plain from the Chalcolithic to the Middle Bronze Age. *BASOR* 269:11–28. https://doi.org/10.2307/1356947

Greenberg R. 2019. *The Archaeology of the Bronze Age Levant: From Urban Origin*. Cambridge. https://doi.org/10.1017/9781316275993

Milevski I. 2009. Local Exchange in the Southern Levant during the Early Bronze Age: A Political Economy Viewpoint. *Antiguo Oriente* 7:125–159.

Milevski I. 2013. The Transition from the Chalcolithic to the Early Bronze Age of the Southern Levant in Socio-Economic Context. *Paléorient* 39/1:193–208. https://doi.org/10.3406/paleo.2013.5495

Milevski I., Liran R. and Getzov N. 2014. The Early Bronze Age Town of Ein Zippori in the Galilee (Israel). *Antiquity* 88/339:2–5. http://antiquity.ac.uk/projgall/milevski339/.

Miroschedji P. de. 2002. The Socio-political Dynamics of Egyptian–Canaanite Interaction in the Early Bronze. In E.C.M. van den Brink and T.E. Levy eds. *Egypt and the Levant: Interrelations from the 4th through the Early 3rd Millennium BCE*. London–New York. Pp. 39–57.

Nickelsberg R. and Shahack-Gross R. 2021. Dor South. *HA–ESI* 133 (September 2). https://www.hadashot-esi.org.il/report_detail_eng.aspx?id=26051&mag_id=133 (accessed May 12, 2024).

Nickelsberg R., Shahack-Gross R. and Yasur-Landau A. 2024. The Early Bronze Age I Coastal Settlements of Israel: A New Phenomenon or a Long-Lived Settlement Tradition? In A. Yasur-Landau, G. Gambash and T.E. Levy eds. *Mediterranean Resilience: Collapse and Adaptation in Antique Maritime Societies*. Sheffield. Pp. 66–91.

Nickelsberg R., Levy T.E., Shahack-Gross R., Tamberino A., McAvoy S., Bermatov-Paz G., Marom N., Arkin Shalev E., Weiss E., Suembikya F. and Yasur-Landau A. 2024. Neolithic Coastal Settlement Continuity in the Face of Climate Change: A Case Study from Habonim North, Israel. *Antiquity* 98/398:343–362. https://doi.org/10.15184/aqy.2024.32

Ogloblin Ramirez I., Galili E., Nickelsberg R., Waiman-Barak P. and Shahack-Gross R. 2021. Appendix to: Pottery from Submerged Neolithic/Early Chalcolithic Settlements off the Carmel Coast, Israel: A Microarchaeological Study of Raw Material Procurement and Firing Technology. *JIPS* 51:130–135.

Ogloblin Ramirez I., Galili E. and Shahack-Gross R. 2021. Pottery from Submerged Neolithic/Early Chalcolithic Settlements off the Carmel Coast, Israel: A Microarchaeological Study of Raw Material Procurement and Firing Technology. *JIPS* 51:105–121.

Orton C., Tyers P. and Vince A. 1993. *Pottery in Archaeology*. Cambridge.

Paz Y. 2002. Fortified Settlements of the EB IB and the Emergence of the First Urban System. *Tel Aviv* 29/2:238–261. https://doi.org/10.1179/tav.2002.2002.2.238

Paz Y. 2023. The Egyptian Enclaving of Southern Canaan during the Late Fourth Millennium BCE: Some Theoretical, Cultural, and Spatial Aspects. *Journal of Ancient Egyptian Interconnections* 37:243–352.

Paz Y., Elad I. and Cohen-Weinberger A. 2021. Three Egyptian *Serekh*-Like Incisions Found on One Vessel at the Early Bronze Age IB City of ‘En Esur, Israel. *Journal of Ancient Egyptian Interconnections* 29:52–66.

Ratzlaff A., Galili E., Waiman-Barak P. and Yasur-Landau A. 2017. The Plurality of Harbors at Caesarea: The Southern Anchorage in Late Antiquity. *JMA* 12/2:125–146. https://doi.org/10.1007/s11457-017-9173-z

Ravikovitch S. 1969. *Soil Map 1:250000, North.* Reḥovot.

Regev J., Miroschedji P. de, Greenberg R., Braun E., Greenhut Z. and Boaretto E. 2012. Chronology of the Early Bronze Age in the Southern Levant: New Analysis for a High Chronology. *Radiocarbon* 54/3–4:525–566. https://doi.org/10.1017/S003382220004724X

Sass E. 1968. Geology of the Umm el-Fahm Area, Northern Israel. *IJES* 17:115–130.

Sass E., Dekel A. and Sneh A. 2013. The Geological Map of Israel, 1:50,000. Sheet 5-II, Umm el-Fahm. In M. Rosensaft. *Vectorial Format of the 1:50,000 Geological Map of Israel.* Jerusalem. https://www.gov.il/he/departments/general/um-el-fahem-map (accessed May 12, 2024).

Shahack-Gross R., Nickelsberg R., Yasur-Landau A., Ogloblin Ramirez I., Pietraszek A., Gur-Arieh S., Marom N., Patania I., Teutch N. and Bermatov-Paz G. 2024. The Early Bronze Age IA Site at Dor South, Carmel Coast, Israel: The Economic System of a Pre-urban Coastal Settlement in the Eastern Mediterranean. *CARMEL: Studies in Archaeological Sciences and Conservation.*

Sharvit J., Galili E., Rosen B. and Brink E.C.M. van den. 2002. Predynastic Maritime Traffic along the Carmel Coast of Israel: A Submerged Find from North ‘Atlit Bay. In E.C.M. van den Brink and E. Yannai eds. *In Quest of Ancient Settlements and Landscapes: Archaeological Studies in Honour of Ram Gophna*. Tel Aviv. Pp. 159–166.

Segev A. and Sass E. 2009. The Geological Map of Israel 1:50,000. Sheet 3-III, Atlit. In M. Rosensaft. *Vectorial Format of the 1:50,000 Geological Map of Israel*. Jerusalem. https://www.gov.il/he/departments/general/atlit-map (accessed May 12, 2024).

Segev A., Sass E., Ron H., Lang B., Kolodny Y. and McWilliams M. 2002. Stratigraphic, Geochronologist, and Paleomagnetic Constraints on Late Cretaceous Volcanism in Northern Israel. *IJES* 51:297–309. https://doi.org/10.1560/VUTP-RNR5-UU08-Y7WT

Sneh A., Sass E., Bein A., Arad A. and Rosensaft M. 1996. The Geological Map of Israel, 1:50,000. Sheet 5-I, Hadera. In M. Rosensaft. *Vectorial Format of the 1:50,000 Geological Map of Israel.* Jerusalem. https://www.gov.il/en/departments/general/hadera-map (accessed May 12, 2024).

Stoops G. 2003. *Guidelines for Analysis and Description of Soil and Regolith Thin Sections.* Madison, Wis.

Waiman-Barak P., Gilboa A. and Goren Y. 2014. A Stratified Sequence of Early Iron Age Egyptian Ceramics at Tel Dor, Israel. *Egypt and the Levant* 24:315–342. https://doi.org/10.1553/s315

Walley C.D. 1997. The Lithostratigraphy of Lebanon: A Review. *Lebanese Science Bulletin* 10/1:81–108.